HUNGARIAN JOURNAL OF
INDUSTRY AND CHEMISTRY
Vol. 53(2) pp. 79–84 (2025)
hjic.mk.uni-pannon.hu
DOI: 10.33927/hjic-2025-21

HUNGARIAN JOURNAL OF INDUSTRY AND CHEMISTRY
HJIC

S-POLARIZED LIGHT-INDUCED UV-VIS PLASMONICS IN Al-Ag DIMERS: A THEORETICAL PERSPECTIVE

RAJU DEVIKA[1], AISWARYA SATHEESH[1], PEARL AUGUSTINE[2], MANOJ PARAMESWARAN[2] AND RANJINI RADHAKRISHNAN[1]*

1 Department of Physics, Kuriakose Elias College, Mannanam, Kottayam, Kerala, 686 561, INDIA
2 Department of Chemistry, St. Michael's College, Cherthala, Alappuzha, Kerala, 688 539, INDIA

The interaction of light with metallic nanoparticle dimers has gained significant attention due to the enhanced local electric fields generated within the nanogap region. In this study, a detailed theoretical investigation of plasmonic homodimers and heterodimers composed of Al and Ag, covering the deep ultraviolet to visible spectral range, is undertaken. Simulations are carried out using COMSOL Multiphysics version 5.6 to examine the effects of dimer composition, gap width and particle size on far-field optical responses. The localized surface plasmon resonance (LSPR) behavior with the systematic variation of dimer radii and interparticle spacing to explore their influence on resonance characteristics is focused on in particular. The results reveal a redshift in LSPR peaks as particle size increases, while a reduction in gap width induces a blueshift. Furthermore, the LSPR wavelength of the Al-Ag heterodimer consistently falls between those of the respective homodimers. These findings demonstrate that the plasmonic response of such dimers can be effectively tuned by adjusting geometric and material parameters, offering potential for tailored nanophotonic applications.

Keywords: dimers, plasmons, nanoparticles, simulation, localized surface plasmon resonance

1. Introduction

The collective oscillatory movements of the conduction band electrons on the metal-dielectric interface when irradiated with light give rise to two pivotal phenomena, surface plasmon resonance (SPR) and localized surface plasmon resonance (LSPR) [1],[2]. Both phenomena arise from the electromagnetic excitation of free electrons in the conduction band of the metal surface. Surface plasmons (SPs) are coherent delocalized electron oscillations that occur at the metal/dielectric interface. In contrast, localized surface plasmons (LSPs) are formed when surface plasmons become confined within nanoparticles whose size is comparable to or smaller than the wavelength of the incident light used to excite the plasmons.

Plasmon resonance occurs when the electromagnetic field of the incident light aligns with the energy of the oscillating electrons on the surface of the nanometallic particles/nanometallic surface, fulfilling the resonance condition. An in-depth knowledge of these systems will greatly benefit the development of various applications, including Surface-Enhanced Raman Spectroscopy (SERS) [3],[4], biological sensing [5], solar cell design [6], photocatalysis [7],[8], pesticide detection [9],[10], toxin monitoring [11],[12] as well as gas and vapor sensing [13],[14].

Noble metallic nanoparticles (NPs) are the widely utilized plasmonic nanomaterials that, upon interaction with incident light, unlock diverse applications known for their reliable performance [15]. Moreover, when two metallic nanoparticles are placed in close proximity to each other (forming a dimer), plasmons in their individual nanostructures couple, leading to plasmon hybridization. The examination of metallic dimers, consisting of two closely spaced metallic nanoparticles, is of great importance in the field of nanoplasmonics [16]. These systems showcase distinctive optical properties because of the robust electromagnetic interplay between the individual nanoparticles. Understanding metallic dimers is vital to implement their potential applications in surface-enhanced spectroscopy, nano-optics and photonic devices. Plasmon hybridization can be used to understand the multifeatured plasmonic response of complex structures [17]. Plasmonic metallic dimers are interesting candidates for a variety of optical and sensing applications as they exhibit a significant degree of plasmonic interaction between two closely spaced nanoparticles [18].

Extensive research has sought to comprehend the mechanisms that govern electromagnetic interactions within metallic dimer systems. The interaction between

Received: 21 July 2025; Revised: 5 Aug 2025;
Accepted: 15 Aug 2025
*Correspondence: ranjinimanoj@kecollege.ac.in

light and metal in addition to further effects which arise because of this interaction is always an interesting topic for scientists. Although the plasmonic properties of noble metals such as silver (Ag) and gold (Au) have been well studied, aluminum (Al) remains the least explored and can be regarded as a viable alternative due to its affordability, abundance and strong plasmonic response in the ultraviolet (UV) spectrum. However, a thorough investigation into the field intensity distribution and hot spot formation in Al nanostructures within the visible region has yet to be comprehensively conducted. In this study, a theoretical investigation of aluminum and silver homodimers is performed followed by an analysis of Al-Ag heterodimers to explore how their plasmonic properties can be tuned. By simulating their response under different conditions, our aim is to understand the impact of material composition on plasmonic resonance behavior. This comparative analysis provides insights into the potential of hybrid plasmonic systems for applications in UV-Vis plasmonics such as sensing and photonic devices. Plasmonic coupling resonances of Ag and Al homodimers as well as Ag-Al heterodimers are evaluated using the simulation software COMSOL Multiphysics version 5.6. The study focuses on how dimer size and the interparticle gap influence the plasmonic resonance wavelength.

2. Computational Methods

Numerical simulations of homo- and heterodimers were carried out using COMSOL Multiphysics version 5.6 which is a powerful simulation software that enables Multiphysics modelling and analysis of complex engineering and scientific problems through finite element methods in a user-friendly, integrated environment [19]. The simulation was conducted by solving the frequency domain form of Maxwell's equations. An s-polarized wave represented by the following wave equation was used:

$$exp(-j_* ewfd.k_{0*}z) \quad (1),$$

where k_0 denotes the propagation constant. Aluminum and silver were selected as representative materials for this study as these metals are promising candidates for supporting plasmons. The material data were selected from the COMSOL database [Al: Rakić 1995: 0.00012399-200 µm and Ag: Werner et al. 2009: n, k 0.01759-2.480 µm]. Spherical nanospheres of identical radius were designed and electromagnetic radiation with an electric field polarized perpendicular to the dimer's axis (s-polarized wave) applied. Air was designated as the surrounding medium for the dimer system and a perfectly matched layer (PML) was implemented to mitigate the backscattering effect. Triangular meshing elements were employed to discretize the external PML surface and the remaining surfaces were discretized using tetrahedral meshing elements, thereby enhancing the degree of accuracy. The far-field extinction cross sections were determined through integrating the time-averaged Poynting vector (S_{ext}) over a surface encompassing the dimer as given in the equation below:

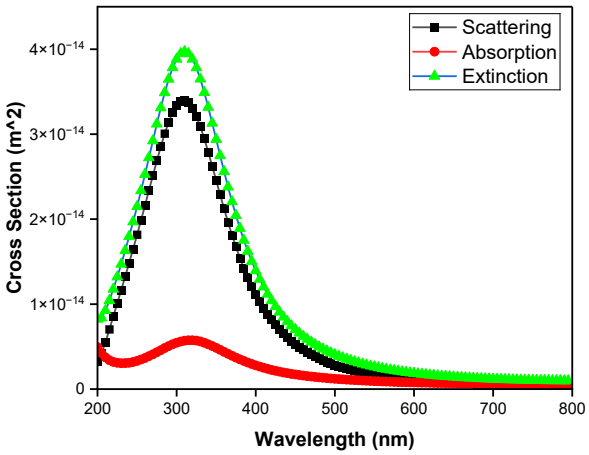

Figure 1: Far field spectra of the Al dimer with a gap size of 2 nm and a radius of 30 nm

$$\sigma_{ext} = \iint -S_{ext}\, ds / I_0 \quad (2),$$

The expression $I_0 = \left|\frac{1}{2} c\varepsilon_0 E_0^2\right|$ represents the power flow per unit area of the incident light. $E_0 = 1$ V/m denotes the amplitude of the incident electric field, ϵ_0 represents the vacuum permittivity and c is the velocity of light. Simulations involved changing the dimer radius while keeping the gap size constant and vice versa. A minimum sub-NP separation of 2 nm was set in this model to avoid quantum tunnelling and non-local effects [20],[21].

3. Results and analysis

The extinction, absorption and scattering cross-sections of the dimer for an s-polarized light wave were analyzed to understand the plasmonic coupling effect. The extinction cross-section of a plasmonic dimer is the sum of its scattering and absorption cross-sections, representing the far-field plasmonic resonance. The scattering, absorption and extinction cross-sections of Al with a radius of 30 nm and a 2 nm gap are depicted in *Figure 1*. The resonance peak of the extinction cross-section was observed at 310 nm within the UV region as already reported in the literature [22]. Furthermore, according to the figure, scattering was more prominent while absorption was minimal.

Furthermore, simulations were conducted by keeping the gap size of the dimer fixed at 2 nm and changing the radius from 30 to 60 nm as presented in *Figure 2*. A redshift of the resonance peak (extinction spectra) was observed upon increasing the radius of the dimer. For a gap of 2 nm and a radius of 30 nm, the resonance wavelength was observed to be 310 nm but shifted to 560 nm as the radius increased to 60 nm. In all Al homodimers, the spectrum was dominated by a pronounced peak of the bonding dipole plasmon mode (BDP). Starting from a radius of 40 nm, the emergence

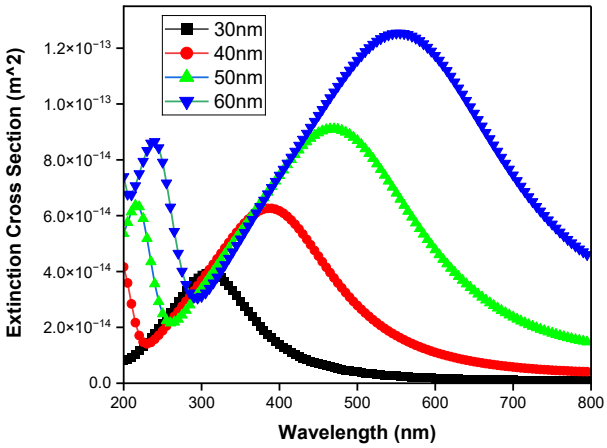

Figure 2: The dependence of the far-field resonance peak on the radius of the Al dimer with a fixed gap size of 2 nm. The far-field extinction spectra exhibit a strong redshift as the radius increases

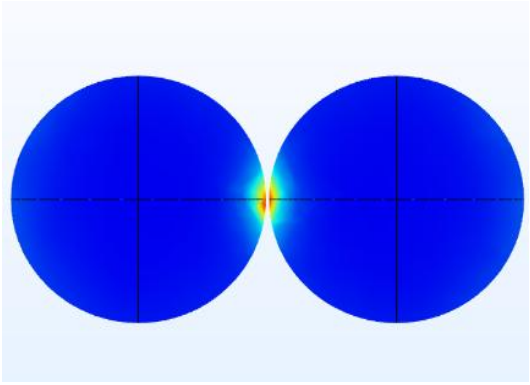

Figure 3: The hot spot formation in the gap of the Al dimer with a radius of 60 nm at a resonance wavelength of 560 nm

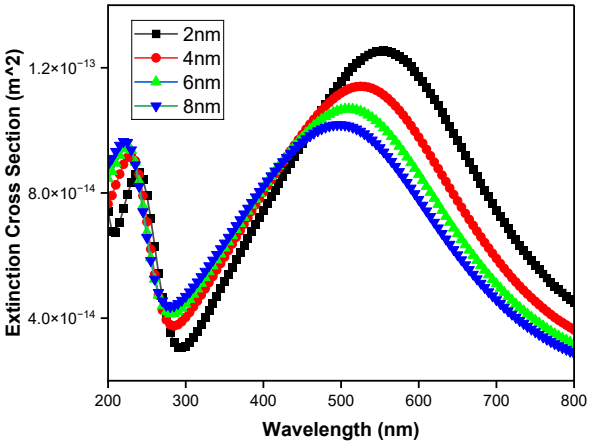

Figure 4: Dependence of the resonance peak on the gap size, that is, 2, 4, 6 and 8 nm, of the Al dimer with a fixed radius of 60 nm

of a second peak at shorter wavelengths was observed. As the dimer size increased, this peak became more pronounced due to the quadrupole plasmon mode (QDP). It was also observed that the intensity of both the BDP and QDP modes increased as the radii increased. BDP, the fundamental mode in a dimer, exhibits a higher extinction cross-section at longer wavelengths compared to other higher order modes that occur at shorter wavelengths. The results show that the plasmonic response of the metallic nanodimer is highly sensitive to its radius. A comparison of the extinction cross-section of various Al homodimers is represented in *Figure 2*. In this study, the extinction cross-sections were compared as they quantify the proportion of incident light that is either scattered or absorbed by the nanodimers. The local electric field distribution near the BDP mode at the resonance peak for Al dimers is illustrated in *Figure 3*.

The extinction spectra of the Al homodimer with a fixed radius of 60 nm and a gap increased from 2 to 8 nm is shown in *Figure 4*. Similar to earlier results, prominent peaks in the BDP mode at longer wavelengths and in the QDP mode at shorter wavelengths were observed. As the gap size was increased, the intensity of the BDP mode decreased, while the QDP mode intensity increased. Both modes were blue shifted as the gap size of the homodimer was increased. It was observed that the corresponding shift in the quadrupole mode was less when compared to the shift in the BDP mode, clearly demonstrating the dependence of the dimer radius and gap size on the plasmonic response of the dimer system to the s-polarized electromagnetic wave.

Similarly, Ag nanodimers were analyzed, yielding far-field extinction spectra for various radii and gap sizes (*Figure 5a*). A redshift was observed when increasing the size of the dimer, similar to the behavior seen in Al dimers at the resonance peaks in the prominent BDP mode. In contrast to the Al homodimers, several higher multipole peaks were detected at shorter wavelengths, however, these higher modes were less pronounced. For the dimer with a radius of 30 nm, only a single higher-order mode was observed in the BDP mode. As the radius increased, more higher modes became apparent, with three higher modes identified for the dimer with a radius of 60 nm. The formation of a hot spot in the gap of a silver (Ag) dimer with a radius of 60 nm at the resonance wavelength is shown in *Figure 5b*.

The far-field spectra regarding different gap sizes for Ag dimers were also computed and presented in *Figure 6*. When the gap size of the dimer was reduced, a blueshift was observed at the resonance peaks in the prominent BDP mode. Unlike the behavior seen with Al homodimers, no shift was detected in the other higher modes, which tended to overlap. To analyze the impact of material properties on the resonance wavelength, the optical plasmonic properties of the Al-Ag heterodimer were also simulated. The far-field optical spectra of the Al-Ag heterodimer are presented in *Figure 7a*. Following the approach of earlier studies, the gap was fixed at 2 nm and the effect of the radius evaluated by increasing it from 30 to 60 nm. At 30 nm, the dominant peak identified as the BDP mode exhibited a significant redshift as the radius increased. A higher-order mode was also observed for the dimer with a radius of 30 nm at shorter wavelengths in the near-UV region, however, became less pronounced as the radius increased. As the particle

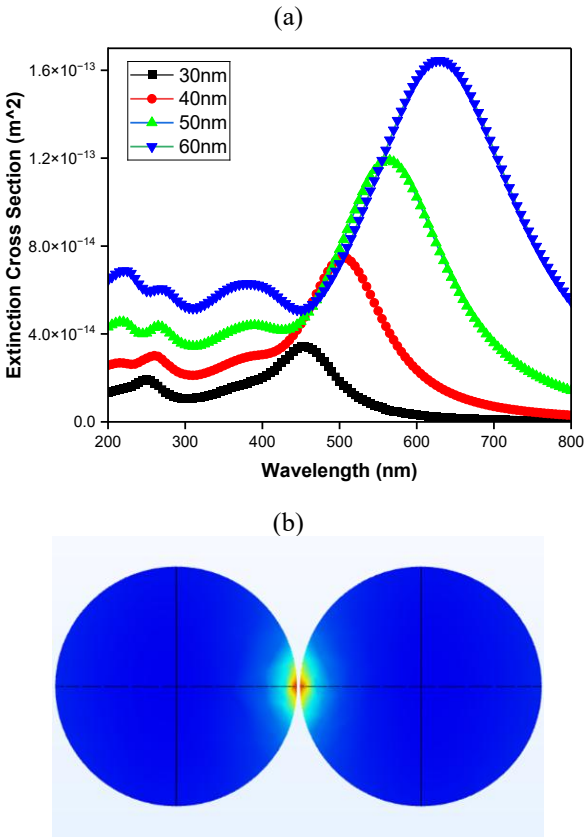

Figure 5: (a) The dependence of the resonance peak on the radius of the Ag dimer with a fixed gap size of 2 nm. The intensity of the redshift increases as the radius increases; (b) Hot spot formation in the gap of the Ag dimer with a radius of 60 nm

size grew, the dipole resonance became more dominant due to the larger scattering cross-section. The far-field optical spectra of the Al-Ag heterodimer with a fixed radius of 60 nm is illustrated in *Figure 7b*. The impact of the gap was assessed by increasing it from 2 to 6 nm, revealing a blueshift at the resonance peaks in the extinction spectra of the prominent BDP mode while only a slight blueshift in the higher order mode was observed.

The relationship between the radii and gap sizes of nanoparticles with their resonance wavelengths for three different dimers, namely the Al-Ag heterodimer as well as Al and Ag homodimers, is illustrated in *Figure 8*. It was observed that as the radius of the nanoparticles increased, the resonance wavelength (corresponding to the BDP mode) also increased. The resonance wavelength of the heterodimer was found to lie between those of the Al and Ag dimers, as shown in *Figure 8.* Consequently, the BDP mode of the heterodimer closely resembled an overlap between the BDP modes of Al and Ag. Furthermore, the BDP modes of the heterodimer tend to align more closely with silver, suggesting that the properties of the heterodimer may more closely resemble a silver homodimer.

Among the three materials considered, the Ag nanoparticle dimer exhibited the longest resonance wavelength followed by the Al-Ag dimer with the Al dimer yielding the shortest. This suggests that Ag

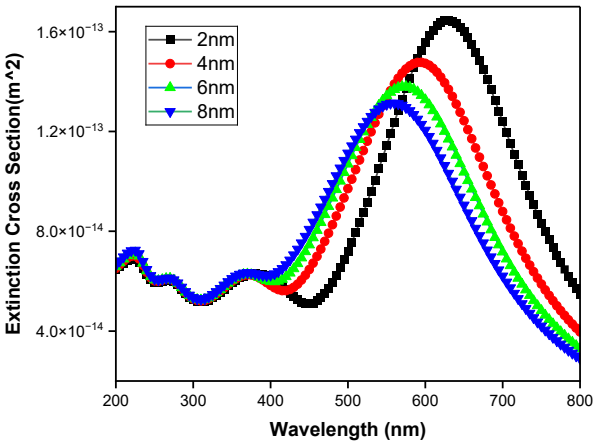

Figure 6: The dependence of the resonance peak on the gap of the Ag dimer with a fixed radius of 60 nm

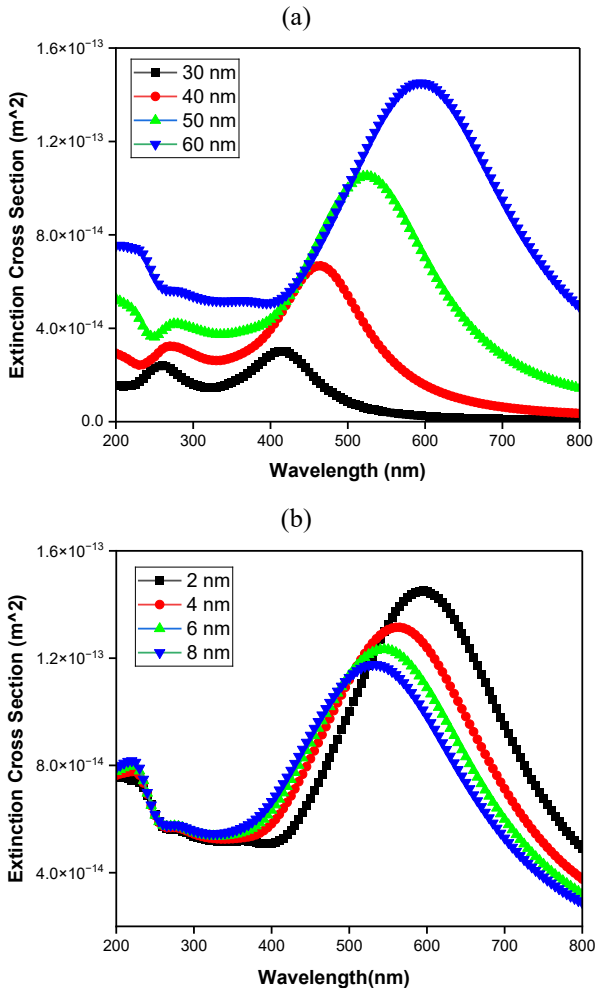

Figure 7: (a) The dependence of the resonance peak on the size of the Al-Ag dimer with a fixed gap of 2 nm. A strong redshift was observed when the radius increased; (b) The dependence of the resonance peak on the gap of the heterodimer with a fixed radius of 60 nm

nanoparticles possess the longest resonance wavelength while Al provides the shortest across the examined wavelength range for any given gap size. The strong

plasmonic response of Ag resulted in higher resonance wavelengths, while the combination of aluminum and silver modifies the plasmonic properties, leading to intermediate resonance wavelengths. Al exhibited the shortest resonance wavelengths due to its distinct properties compared to those of silver.

4. Conclusions

A more profound understanding of light-matter interactions has paved the way for "plasmonics" to develop into a rapidly advancing field with a wide range of innovative applications. Plasmonic coupling in Al and Ag homodimers as well as in the Al-Ag heterodimer was analyzed using COMSOL Multiphysics version 5.6 simulation software with the incident light polarized along the dimer axis using various radii and gap sizes. A redshift as the radii increased and blueshift as the gap size increased was observed in all configurations of dimer. Regarding Ag and Al-Ag dimers, a larger particle size potentially diminished the quadrupole peak while the opposite effect occurred in the Al homodimer. For nearly all configurations of dimers, multipole peaks were observed in the QDP and BDP modes towards the lower and longer wavelengths, respectively. In aluminum homodimers, as the particle size increased, a prominent peak appeared in the near-UV range, suggesting the presence of strong quadrupole modes. In the case of the heterodimer, multipole peaks appeared only at radii of 30 and 40 nm but disappeared at larger radii accompanied by a broadening in the BDP mode.

Concerning the relationship of the radii and gap size of nanoparticles with their resonance wavelengths with regard to three different dimers, it was found that the resonance wavelength of the heterodimer fell between Al and Ag in both cases. The strong plasmonic response of Ag results in longer resonance wavelengths, while the combination of aluminum and silver modifies the plasmonic properties, leading to intermediate resonance wavelengths. Al exhibits shorter plasmonic resonance wavelengths due to its distinct properties compared to those of silver. This study shows how the interaction between light and nanoparticles can be controlled or modified based on their arrangement. This means that by modifying the configuration of nanoparticles (dimers), optical properties such as scattering, absorption, or resonance behavior can be fine-tuned. Theoretical studies show that Al stands out as one of the rare metals capable of achieving plasmonic resonance across a wide spectral range from near-ultraviolet to visible simply by adjusting the particle size and interparticle distance. This is significant in nanophotonics, perhaps leading to more precise control over light-matter interactions for applications in sensing, imaging and the development of other optical devices.

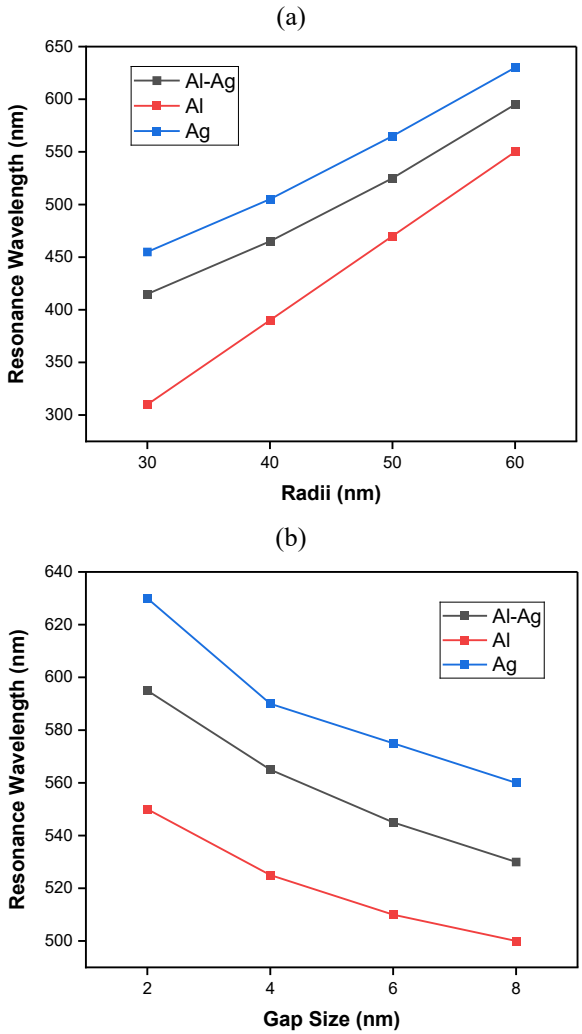

Figure 8: The relationship of the resonance wavelength with (a) the radii and (b) gap size of the three different dimers, namely the Al-Ag heterodimer as well as Al and Ag homodimers

Acknowledgements

The authors are grateful for the financial support provided by the Department of Science and Technology - Science and Engineering Research Board (SERB/SB/S1/PC-42/2012), the DST-FIST program by the Indian Government as well as I-STEM for providing access to the COMSOL Multiphysics version 5.6 simulation software.

REFERENCES

[1] Ritchie, R.H.: Plasma losses by fast electrons in thin films, *Phys. Rev.*, 1957, **106**(5), 874–881, DOI: 10.1103/PhysRev.106.874

[2] Kelly, K.L.; Coronado, E.; Zhao, L.L.; Schatz, G.C.: The optical properties of metal nanoparticles: The influence of size, shape, and dielectric environment, *J. Phys. Chem. B*, 2003, **107**(3), 668–677, DOI: 10.1021/jp026731y

[3] Sharma, B.; Frontiera, R.R.; Henry, A.-I.; Ringe, E.; Van Duyne, R.P.: SERS: Materials, applications, and the future, *Mater. Today*, 2012, **15**(1-2), 16–25, DOI: 10.1016/S1369-7021(12)70017-2

[4] Ding, S.-Y.; Yi, J.; Li, J.-F.; Ren, B.; Wu, D.-Y.; Panneerselvam, R.; Tian, Z.-Q.: Nanostructure-based plasmon-enhanced Raman spectroscopy for surface analysis of materials, *Nat. Rev. Mater.*, 2016, **1**(6), 16021, DOI: 10.1038/natrevmats.2016.21

[5] Weller, L.; Thacker, V.V.; Herrmann, L.O.; Hemmig, E.A.; Lombardi, A.; Keyser, U.F.; Baumberg, J.J.: Gap-dependent coupling of Ag-Au nanoparticle heterodimers using DNA origami-based self-assembly, *ACS Photonics*, 2016, **3**(9), 1589–1595, DOI: 10.1021/acsphotonics.6b00062

[6] Atwater, H.A.; Polman, A.: Plasmonics for improved photovoltaic devices, *Nat. Mater.*, 2010, **9**(3), 205–213, DOI: 10.1038/nmat2629

[7] Verbruggen, S.W.; Keulemans, M.; Goris, B.; Blommaerts, N.; Bals, S.; Martens, J.A.; Lenaerts, S.: Plasmonic 'rainbow' photocatalyst with broadband solar light response for environmental applications, *Appl. Catal. B: Environ.*, 2016, **188,** 147–153, DOI: 10.1016/j.apcatb.2016.02.002

[8] Devi, L.G.; Kavitha, R.: A review on plasmonic metal TiO_2 composite for generation, trapping, storing and dynamic vectorial transfer of photogenerated electrons across the Schottky junction in a photocatalytic system, *Appl. Surf. Sci.*, 2016, **360,** 601–622, DOI: 10.1016/j.apsusc.2015.11.016

[9] Lin, T.-J.; Huang, K.-T.; Liu, C.-Y.: Determination of organophosphorous pesticides by a novel biosensor based on localized surface plasmon resonance, *Biosens. Bioelectron.*, 2006, **22**(4), 513–518, DOI: 10.1016/j.bios.2006.05.007

[10] Wang, K.; Wang, Y.; Li, Q.; Liu, Z.; Liu, S.: A fluorescence and localized surface plasmon resonance dual-readout sensing strategy for detection of acetamiprid and organophosphorus pesticides, *Sens. Actuators B: Chem.*, 2022, **351**, 130977, DOI: 10.1016/j.snb.2021.130977

[11] Loiseau, A.; Zhang, L.; Hu, D.; Salmain, M.; Mazouzi, Y.; Flack, R.; Liedberg, B.; Boujday, S.: Core–shell gold/silver nanoparticles for localized surface plasmon resonance-based naked-eye toxin biosensing, *ACS Appl. Mater. Interfaces*, 2019, **11**(50), 46462–46471, DOI: 10.1021/acsami.9b14980

[12] Brahmkhatri, V.; Pandit, P.; Rananaware, P.; D'Souza, A.; Kurkuri, M.D.: Recent progress in detection of chemical and biological toxins in water using plasmonic nanosensors, *Trends Environ. Anal. Chem.*, 2021, **30**, e00117, DOI: 10.1016/j.teac.2021.e00117

[13] Kreno, L.E.; Hupp, J.T.; Van Duyne, R.P.: Metal–organic framework thin film for enhanced localized surface plasmon resonance gas sensing, *Anal. Chem.*, 2010, **82**(19), 8042–8046, DOI: 10.1021/ac102127p

[14] Bingham, J.M.; Anker, J.N.; Kreno, L.E.; Van Duyne, R.P.: Gas sensing with high-resolution localized surface plasmon resonance spectroscopy, *J. Am. Chem. Soc.*, 2010, **132**(49), 17358–17359, DOI: 10.1021/ja1074272

[15] Radhakrishnan, R.; Parameswaran, M.; Kumar, K.S.: The evolution and recent research trends of Surface Enhanced Raman Scattering sensors using plasmonics: Citation network analysis, *Mater. Chem. Phys.*, 2023, **296**, 127255, DOI: 10.1016/j.matchemphys.2022.127255

[16] Burrows, C.P.; Barnes, W.L.: Large spectral extinction due to overlap of dipolar and quadrupolar plasmonic modes of metallic nanoparticles in arrays, *Opt. Express*, 2010, **18**(3), 3187–3198, DOI: 10.1364/OE.18.003187

[17] Prodan, E.; Radloff, C.; Halas, N.J.; Nordlander, P.: A hybridization model for the plasmon response of complex nanostructures, *Science*, 2003, **302**(5644), 419–422, DOI: 10.1126/science.1089171

[18] Katyal, J.: Plasmonic coupling in Au, Ag and Al nanosphere homo-dimers for sensing and SERS, *Adv. Electromagn.*, 2018, **7**(2), 83–90, DOI: 10.7716/aem.v7i2.563

[19] Lahcene, A.; Benamara, N.; Benguediab, M.; Benazza, A.: Efficiency improvements of solar collectors by turbulence promoters, *Hung. J. Ind. Chem.*, 2024, **52**(2), 1–9, DOI: 10.33927/hjic-2024-13

[20] Zuloaga, J.; Prodan, E.; Nordlander, P.: Quantum description of the plasmon resonances of a nanoparticle dimer, *Nano Lett.*, 2009, **9**(2), 887–891, DOI: 10.1021/nl803811g

[21] Zhu, W.; Crozier, K.B.: Quantum mechanical limit to plasmonic enhancement as observed by surface-enhanced Raman scattering, *Nat. Commun.*, 2014, **5,** 5228, DOI: 10.1038/ncomms6228

[22] Ekinci, Y.; Solak, H.H.; Löffler, J.F.: Plasmon resonances of aluminum nanoparticles and nanorods, *J. Appl. Phys.*, 2008, **104**(8), 083107, DOI: 10.1063/1.2999370